JOURNAL OF GEOPHYSICAL RESEARCH, VOL. 106, NO. A6, PAGES 10,625–10,634, JUNE 1, 2001

Processes associated with particle transport in corotating interaction regions and near stream interfaces

D. S. Intriligator,[1] J. R. Jokipii,[2] T. S. Horbury,[3] J. M. Intriligator,[1] R. J. Forsyth,[3] H. Kunow,[4] G. Wibberenz,[4] and J. T. Gosling[5]

Abstract. Pioneer and Ulysses observations of energetic particles and solar wind plasma and magnetic fields are analyzed to study particle transport in corotating interaction regions (CIRs) and near stream interfaces (SIs). Energetic particle diffusion with a lowered coefficient near the SIs as compared with the free solar wind may account for the energetic particle profiles in CIRs and for the modulation of Jovian electrons. Our analyses include examination of the magnetic power and variances perpendicular and parallel to the magnetic field for a range of wave numbers and for a range of conditions within two CIRs. Since the magnetic field immediately on either side of a SI, but near it, is not connected to either the forward shock or reverse shock, it is the cross-field motion of the energetic particles that is relevant. Since the cross-field transport is thought to be related to field line mixing, or random walk, we examined magnetic field fluctuations normal to the average field to determine whether any signature of reduced perpendicular particle transport could be found. Evidence consistent with reduced particle transport near the SI was indeed found when we examined time series of the 1-min averages of the magnetic field components. A planar magnetic structure was associated with the trailing unshocked layer following the SIs (i.e., SI to SI + 12 hours) and also with the entire CIRs, but it was not present in the free solar wind. We have quantitatively examined the effects of shear and compression on particle transport and conclude that the effects of shear and compression reduce particle transport in CIRs and in the vicinity of SIs.

1. Introduction

The reverse shock in a corotating interaction region (CIR) is a prolific source of energetic ions. It can accelerate solar wind suprathermal ions and interstellar pickup ions from keV to MeV energies. Transport processes associated with the magnetic field within CIRs then distribute the accelerated ions in a characteristic way in space. Energetic particle diffusion with a lowered coefficient near the stream interface (SI) as compared with the free solar wind may account for the energetic particle profiles in CIRs and for the CIR modulation of Jovian electrons [*Conlon*, 1978]. *Dwyer et al.* [1997] presented evidence for nonfield-aligned transport in CIRs. The SI lies at the foot of the energetic particle intensity peak associated with the reverse shock *[Intriligator and Siscoe*, 1994, 1995; *Intriligator et al.*, 1995]. Figure 1 shows the typical CIR solar wind speed, specific entropy, and energetic particle profiles for a CIR observed by Pioneer 11 (Bartels Solar Rotation 1923) in 1974 near solar minimum when recurring high-speed streams were present in the solar wind, similar to those observed in 1992-1993 by Ulysses. The solar wind speed in Figure 1 (top) shows distinct forward and reverse shocks. The stream interface is defined by an abrupt increase in the specific entropy argument ($T/n1/2$ with temperature T in kelvins and density n in cm^{-3}; see *Siscoe and Intriligator* [1993], as shown in the Figure 1 (second panel). Figure 1 (bottom) shows energetic-ion data from three instruments indicating that the stream interface is a structural boundary to the energetic particles associated with the reverse shock [*Intriligator and Siscoe*, 1994, 1995; *Intriligator et al.*, 1995].

Since the field lines corresponding to the average field on either side of the stream interface are not connected to either the leading forward shock or the trailing reverse shock [*Palmer and Gosling*, 1978; *Pizzo*, 1989; *Hu*, 1993], it is the cross-field transport (in this paper we define cross-field transport as transport normal to the average magnetic field) of the energetic particles that is relevant to the energetic particle flux profiles in the vicinity of the stream interface [*Intriligator and Siscoe*, 1995]. *Intriligator and Siscoe* [1995] used a Green's function solution to the convection-diffusion equation applied to idealized CIR geometry and found that cross-field transport by stochastic diffusion at a rate that applies to the ambient (free) solar wind would fill the trailing unshocked layer (i.e., the TUL (see below)) adjacent to the stream interface and that there would be no valley in energetic particle intensity there. A reduction of ~2 orders of magnitude was needed in the cross-field transport as

[1]Space Plasma Laboratory, Carmel Research Center, Santa Monica, California.
[2]Department of Planetary Science, University of Arizona, Tucson, Arizona.
[3]The Blackett Laboratory, Imperial College, London, England, United Kingdom.
[4]Extraterrestrische Physik, University of Kiel, Kiel, Germany.
[5]Los Alamos National Laboratory, Los Alamos, New Mexico.

Paper number 2000JA000070.
0148-0227/01/2000JA000070 $09.00

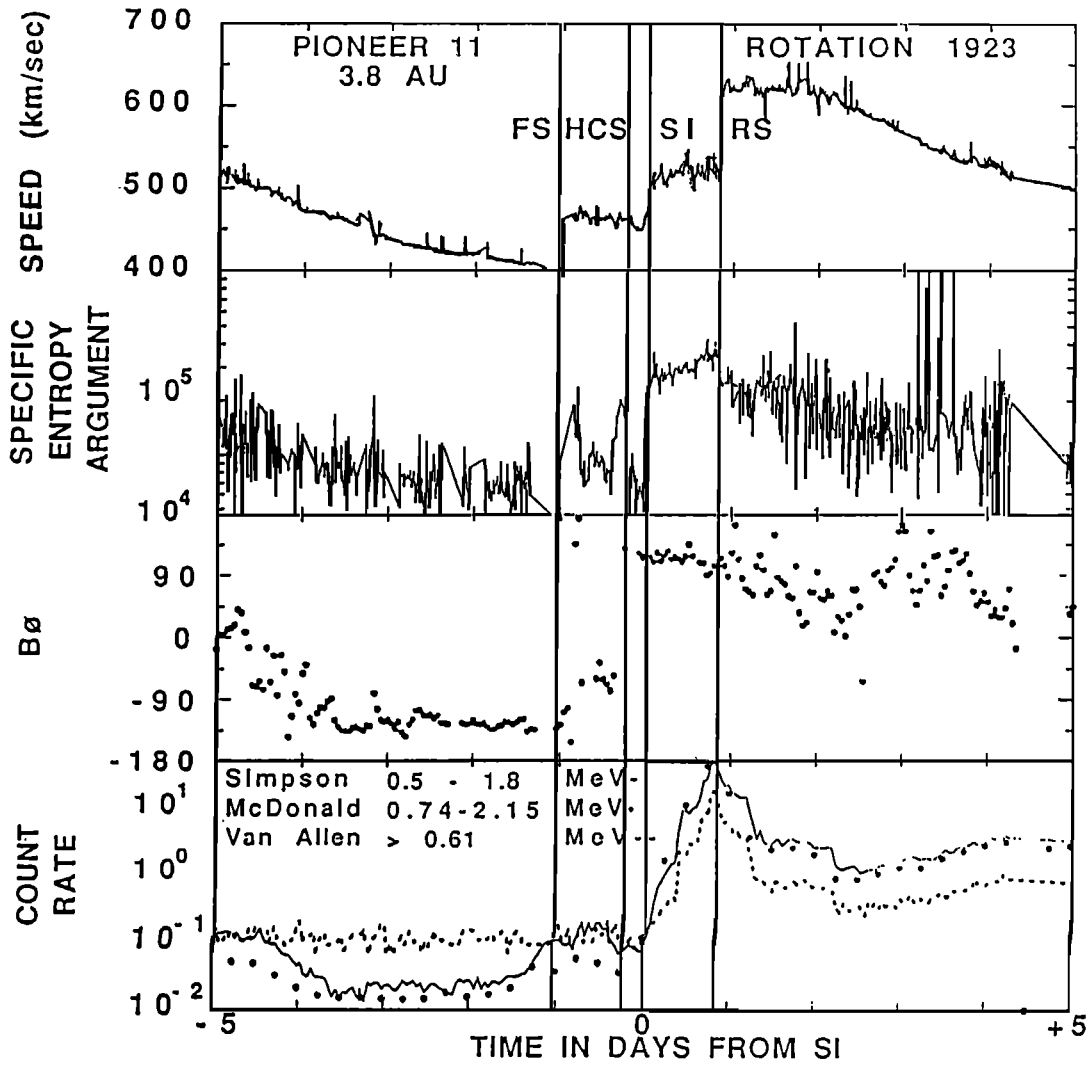

Figure 1. Corotating interaction region (CIR) parameters for Bartels Solar Rotation 1923 as seen at Pioneer 11 at 3.8 AU [*Intriligator and Siscoe*, 1994]. Abbreviations refer to the following: FS, forward shock; HCS, heliospheric current sheet; SI, stream interface; and RS, reverse shock. The "specific entropy argument" plotted in the second panel is $T/n^{\gamma-1}$ or $T/n^{1/2}$ with temperature T in kelvins and density n in cm^{-3}. Specific entropy is proportional to the log of this quantity. The polytropic index γ is taken to be 3/2, because this gives a good fit to the requirement that the specific entropy remain constant with distance [see *Siscoe and Intriligator*, 1993].

compared to that in the free solar wind. Since the cross-field transport is thought to be related to field line mixing or random walk of field lines, in the present study we examined the magnetic field fluctuations normal to the average magnetic field direction to determine whether any signature of reduced perpendicular particle transport could be found. Since these analyses (see below) indicated enhanced levels of fluctuations near the stream interface, the high time resolution time series of the field was examined. These studies showed that near the stream interface there were sharp transitions in the field, often in the component normal to the ecliptic plane. These and other features can be shown to be consistent with reduced random walk of magnetic field lines near the stream interface. This is described qualitatively in section 4 and then quantitatively in section 5.

2. Field Fluctuations

Figure 2 shows, for Ulysses CIR 10, the perpendicular power and the parallel power in the field [*Horbury and Schmidt*, 1999] for wave numbers from 1.6×10^{-5} to 3.2×10^{-5}/km, although results were similar over a wide range of scales. The perpendicular power is elevated in the CIR, and there is no significant drop in this power adjacent to the stream interface. In this paper the LUL and TUL regions denote the leading unshocked layer and the trailing unshocked layer, respectively. In the LUL (TUL) there are no field lines connected with the forward (reverse) shock. For this CIR the duration of the TUL region shown in Figure 2 is ~14 hours [*Intriligator et al.*, 1995]. This Ulysses CIR was analyzed by *Intriligator et al.* [1995] and was found to be similar to the Pioneer CIRs studied by *Intriligator and Siscoe* [1994].

Figure 3a shows the low frequency variances in the three components B_R (top panel), B_T (second panel), and B_N (third panel) of the magnetic field measured at Pioneer 11 during SR 1923 (see Figure 1). The bottom panel shows the magnetic field magnitude. Figure 3b shows the corresponding normalized variances during this time. These

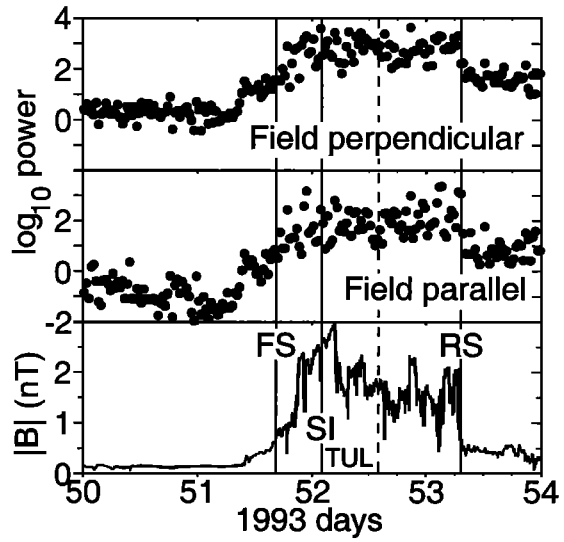

Figure 2. Magnetic field perpendicular power and parallel power for Ulysses CIR10 for the wave number range 1.6×10^{-5} to 3.2×10^{-5}/km. The field magnitude is shown in the bottom panel. TUL denotes the trailing unshocked layer (see text). The perpendicular power is relatively constant across the stream interface. Similar results were found for other wave number ranges (see text).

variances were computed by obtaining 2-hour averages of the direction of the magnetic field vector and then calculating 1-min variances of the field components with respect to this 2-hour average vector. The normalized variances were computed by dividing these quantities by the corresponding field magnitudes. The variances perpendicular to the field (i.e., the normal variances in Figures 3a and 3b, third panel) both show an increase near the stream interface. On the face of it these increases in the normal variances suggest that the random walk of field lines is enhanced, not decreased, near the SI.

Nonetheless, since the energetic particle intensity profiles show a decrease in the vicinity of the stream interface, further investigation of the field seemed warranted. To this end the 1-min averages of the field were examined around the time of the stream interface shown in Figures 3a and 3b. Figure 4 displays the 1-min averages of the B_R, B_T, and B_N components of the field and the field magnitude B. The B_R, B_T, and B_N components are with respect to the R,T,N standard Pioneer coordinate system oriented in space and not with respect to the average field direction as employed in Figures 3a and 3b. Note that in Figure 4 there are large data gaps before the SI.

The B_N fluctuations near the SI in Figure 4 consist of large, rapid changes in the field perpendicular to the ecliptic plane. These large excursions in the field fully explain the elevated perpendicular power near the SI for this case and the large normal variances in the field near the SI shown in Figures 3a and 3b (third panel). They also indicate that, in the vicinity of the SI, it is not particularly meaningful to determine 2-hour average field directions since the field is varying significantly on timescales of several minutes. These rapid variations in the field can be related to a reduction of the random walk of field lines, as is demonstrated below.

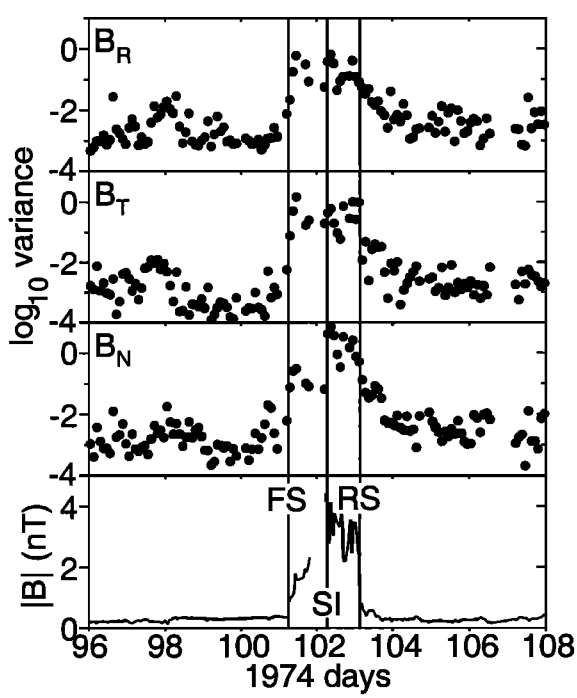

Figure 3a. Low-frequency variances in the three magnetic field components (top panel) B_R , (second panel) B_T , and (third panel) B_N as measured at Pioneer 11 during Bartels SR 1923 (see Figure 1). The bottom panel shows the field magnitude.

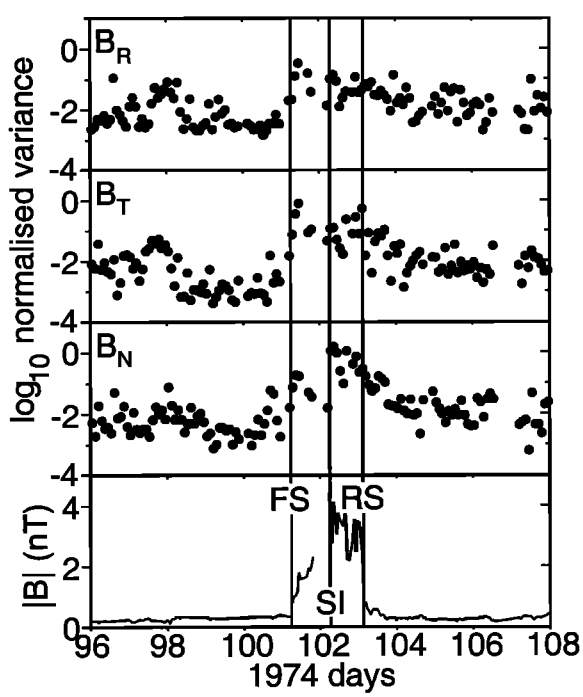

Figure 3b. Corresponding normalized variances for the components shown in Figure 3a. The variances perpendicular to the field both show increases near the stream interface.

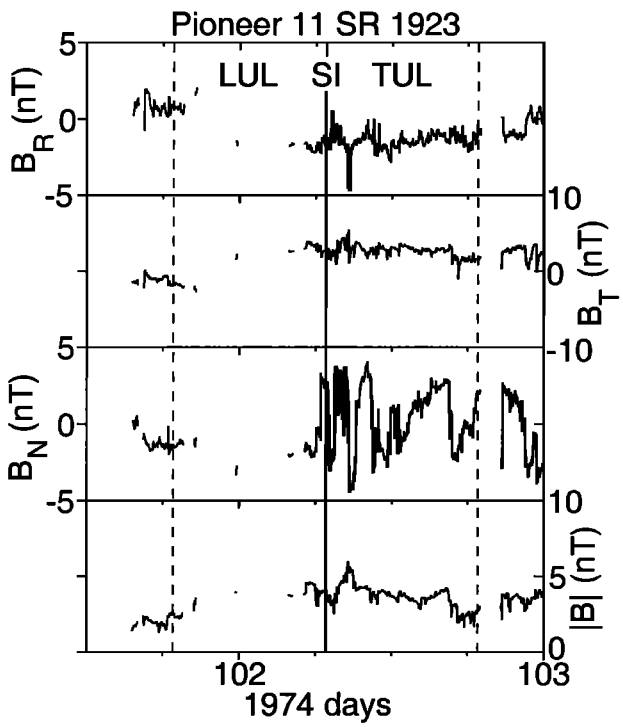

Figure 4. One-minute averages of the magnetic field magnitude and components near the stream interface (SI) for Pioneer 11 Bartels SR 1923 (see Figures 1 and 3a - 3b). The LUL and TUL denote the leading and trailing unshocked layers, respectively. Note the large rapid changes in B_N near the SI.

3. Planar Magnetic Structures

Since our examination of the field fluctuations near the SI indicated large rapid fluctuations perpendicular to the ecliptic plane, we tested for planar magnetic structures near the SI. During a planar magnetic structure (PMS) the magnetic field vectors tend to lie close to a plane [*Nakagawa et al.*, 1989; *Neugebauer et al.*, 1993]. The normal to the plane that defines these events is simply the minimum variance direction.

For the Pioneer events, 1-min averaged field data were

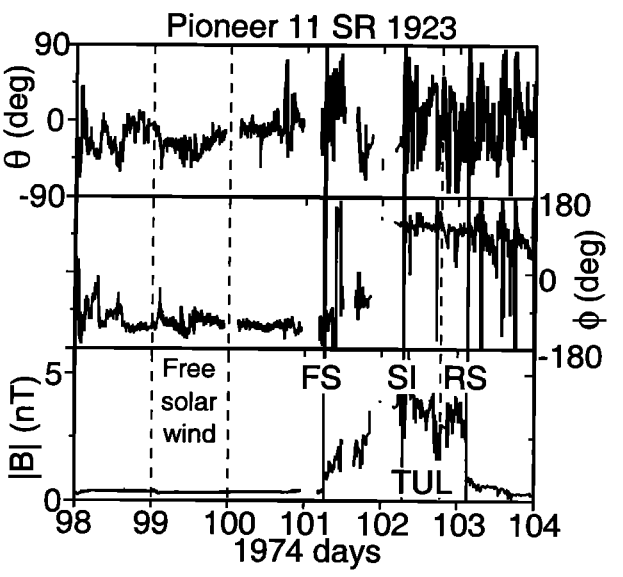

Figure 5a. Interplanetary magnetic field (IMF) data for the CIR of Bartels SR 1923.

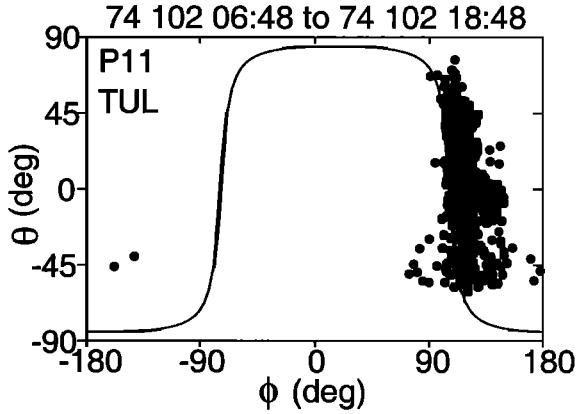

Figure 5b. Scatterplot of the latitude θ versus longitude φ angles of the magnetic field for the TUL (SI to SI + 12 hours). The results for the TUL (SI to SI + 12 hours) indicate that the TUL is a planar structure (see text).

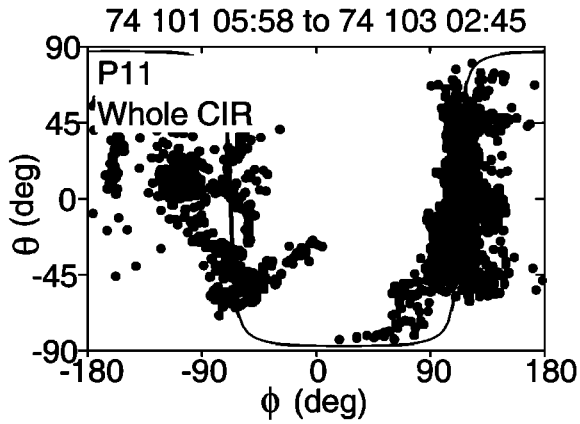

Figure 5c. Results for the whole CIR. The CIR starts at the initial jump in IMF magnitude at the FS and ends at the sharp drop at the RS. The whole CIR also is a planar structure (see text).

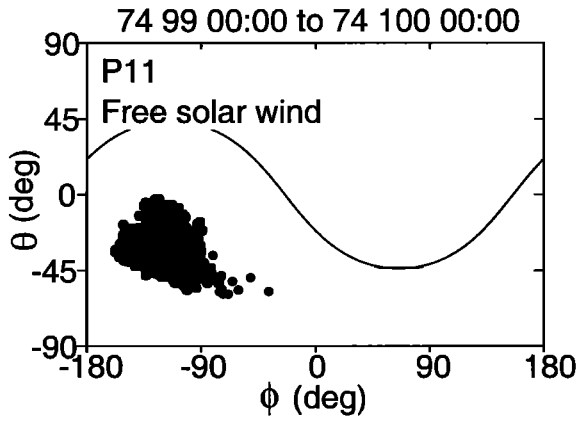

Figure 5d. Results in the free solar wind indicating that this time period is not associated with a planar structure.

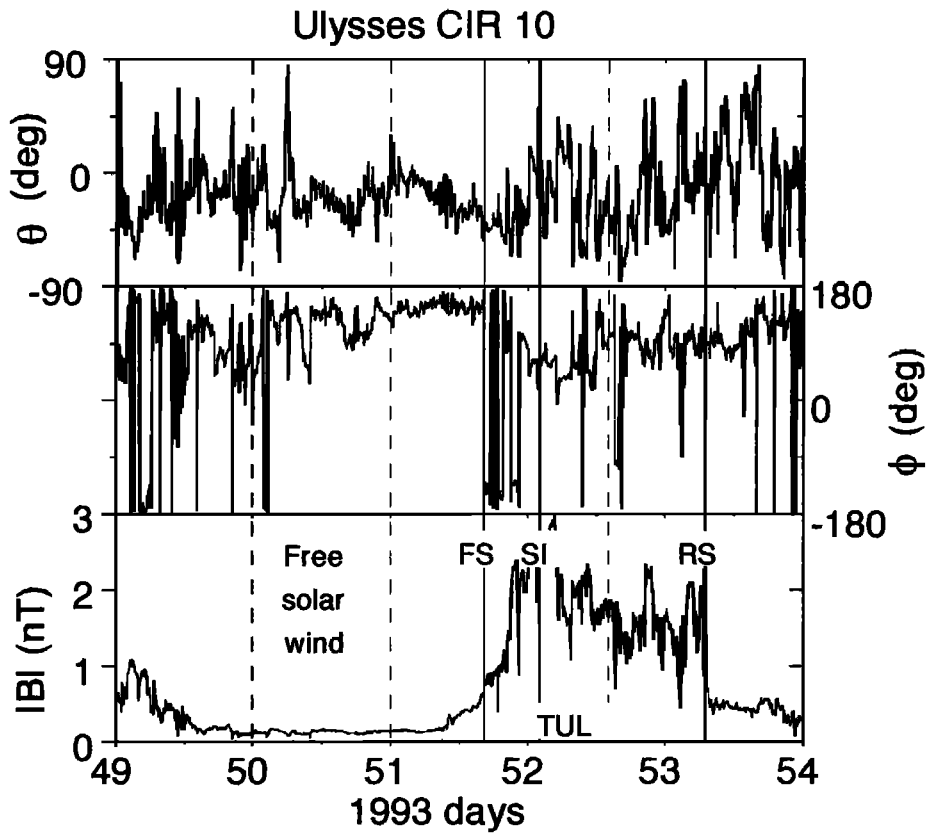

Figure 6a. Same as Figure 5a, but for Ulysses CIR 10.

used; for Ulysses; 5-min averaged data were used to construct scatterplots of the latitude θ versus longitude φ of the magnetic field. For the Pioneer 11 Bartels SR 1923 case shown in Figures 1, 3a, 3b, and 4 we performed the analyses for three time intervals (see Figure 5a); (1) for the TUL, the 12-hour interval starting at the SI (day 102, 0648 to 1848 UT); (2) for the entire CIR (day 101, 0558: 44 UT to day 103, 0245: 47 UT); and (3) outside the CIR (most of day 99). These scatterplots are shown in Figures 5b, 5c, and 5d, respectively. Figure 5b shows the θ-φ plot for the TUL. It is clear that the data points lie on a portion of the solid line, which corresponds to the orientation of the planar structure. This indicates that the TUL lies along one sector (~+90°) and that it is a planar structure. The normal of the plane is oriented at theta = -4.6°, φ = 14.2°, and the intermediate to minimum eigenvalue ratio (int/min) equals 2.9. Such a large value indicates that field vectors tend to lie close to a plane. In essence, Figure 5b shows that most of the field variations are perpendicular to the compression plane of the CIR, which is itself parallel to the SI.

To further examine the PMS structure associated with the CIR, Figure 5c shows the θ-φ plot for the whole CIR. Again, it is clearly planar but for the entire CIR two sectors (~-90° and +90°), are observed although in this case the "tilt" of the structure is small.

To check our PMS results and their implications for cross-field diffusion for the TUL (and whole CIR), we performed a similar analysis for a time interval outside the CIR (see Figure 5d). Unlike the results of Figure 5b (and 5c), it is clear that no planar structure is present here, thus verifying the difference between the TUL (and CIR) and the outside region.

We obtain similar results for the Ulysses CIR 10 (see Figure 2) as shown in Figures 6a - 6d, which are similar in format to Figures 5a - 5d. Figure 6a shows the time interval around CIR 10 in 1993. Here again we performed the analyses for three different time intervals: (1) in the TUL from SI to SI + 12 hours (day 52, 0200 to 1400 UT) *Intriligator et al.* [1995] estimated that at this latitude the total duration of the TUL was ~14 hours; for the purposes of our PMS analysis we chose to use a 12-hour interval trailing the SI at Ulysses to be the same length as the interval chosen for Pioneer 11); (2) for the entire CIR (day 51, 1002: 30 UT to day 53, 0702: 30 UT); and (3) outside the CIR in the free solar wind (~day 50). The θ-φ plot in Figure 6b for the 12 hours in the TUL shows the data following the line and the planar structure of the TUL. For this TUL the orientation of the planar structure is θ equals 31.6°, φ equals 37.6°, and the int/min ratio equals 4.8. Figure 6c demonstrates the planar structure for the whole CIR, and Figure 6d shows that there is no planar structure in the interval outside the CIR. We note that our results for the whole CIR in Figure 6c are similar to those of *Clack et al.* [2000], who used Ulysses data to study two entire CIRs.

Figures 7 and 8 show for Pioneer 11 and Ulysses, respectively, a calculation of the magnetic field power in three directions: parallel to the planar magnetic structure plane normal (the squares); perpendicular to the PMS plane normal and perpendicular to the local mean magnetic field (circles); and perpendicular to the first two directions (triangles). This was done for 2-hour intervals. In and near the TUL the power is highest in the direction perpendicular to the PMS plane normal and perpendicular to the local mean

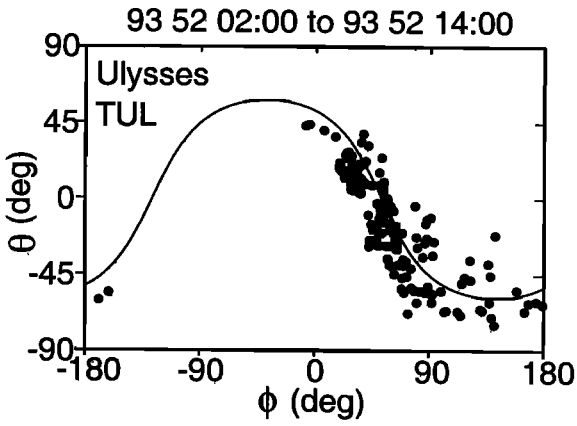

Figure 6b. Same as Figure 5b, but for Ulysses CIR 10.

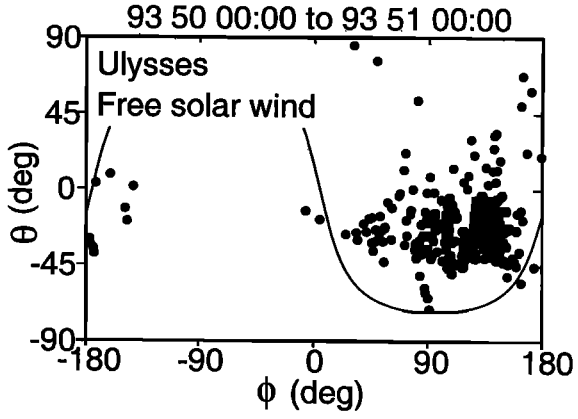

Figure 6d. Same as Figure 5d, but for Ulysses CIR 10.

magnetic field observed at Pioneer 11. Similar results are obtained in and near the TUL for the Ulysses case, shown in Figure 8.

4. Discussion

The contribution of field line braiding or random walk to the particle diffusion results from particles tending to follow the randomly varying component of the magnetic field normal to the mean field (see Figure 9). More precisely, it is the angle of the instantaneous field relative to the average field direction that is relevant, since that determines the particle motion normal to the average field.

First, we consider a situation where there is a local current sheet, in which the field changes its direction abruptly as a function of distance normal to the sheet. In this case, simple geometric considerations show that the magnetic field mixing or random walk cannot extend across the current sheet. In addition, it can be shown that other common situations in the flow also reduce the random walk.

Consider a region where there is a shear in the fluid motion caused primarily by a change in the velocity of the flow (see Figure 10). From the fact that the magnetic field is frozen into the flow, it is easy to show that, in general, the shear amplifies the component of the magnetic field parallel to the shear plane and in the direction of the flow, while leaving the field component normal to the shear plane unaffected. The field becomes stretched and large in the shear plane, and the field normal to that plane remains the same. This produces a change in field direction within the shear layer and reduces the perpendicular random walk and diffusion coefficient, by an amount which scales with the square of this angle.

Similarly, if we consider an approximately planar region where the fluid is compressed, in a direction roughly normal to the average magnetic field, the compression can readily be shown to increase the magnetic field component normal to the flow (or parallel to the average field), while not changing the component perpendicular to the average field. Again, as for shear, the angle between the average field and the local field is decreased by the process, reducing the field line random walk and hence the perpendicular diffusion.

From these considerations we see that a local reduction of

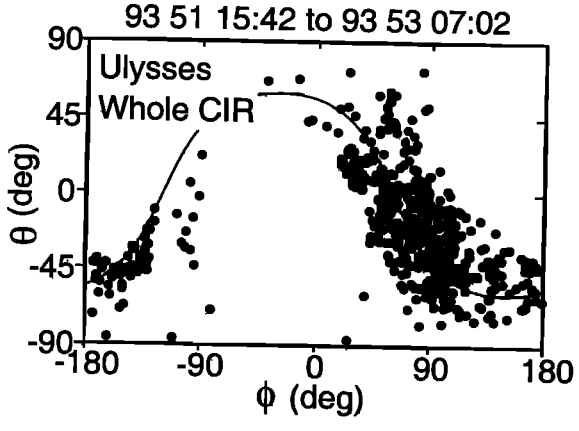

Figure 6c. Same as Figure 5c, but for Ulysses CIR 10.

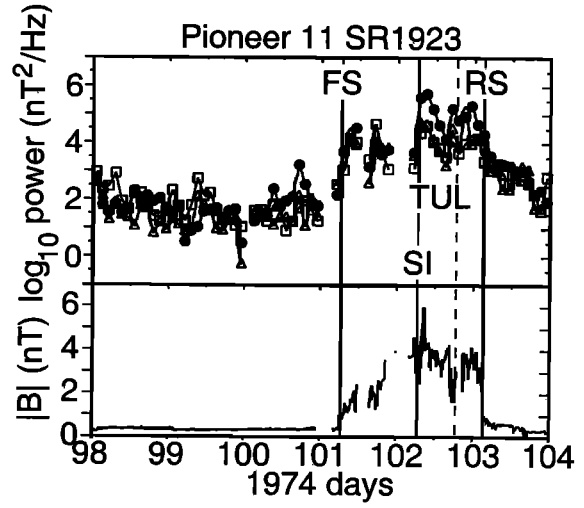

Figure 7. Calculation for Pioneer 11 SR 1923 of the magnetic field power in three directions associated with the PMS and the local magnetic field: parallel to the PMS plane normal (squares); perpendicular to the PMS plane normal and to the local mean magnetic field (circles), and perpendicular to the first two directions (triangles). Note in and near the TUL, the elevated power perpendicular to the PMS planes normal to the local mean magnetic field.

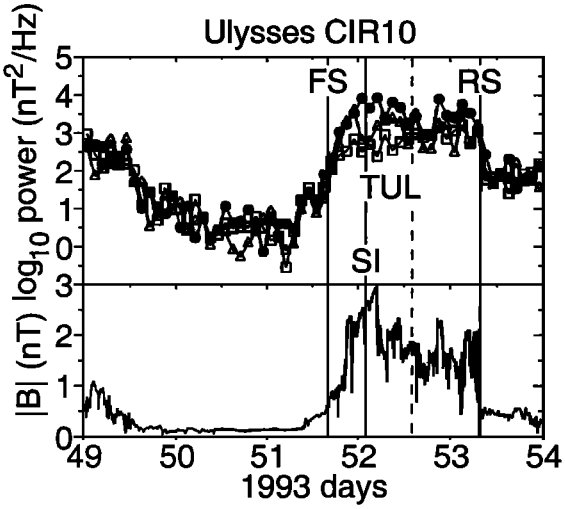

Figure 8. Same as Figure 7, but for Ulysses CIR 10.

field line random walk, and hence perpendicular diffusion, can occur in relatively common flow situations. These would produce a reduction of particle transport across the magnetic field in the associated planar regions of space.

We also point out that in both of the cases discussed above, since the initial parallel field is amplified, any loops or reversals, which may well be present initially, will also be amplified, producing larger and sharper jumps in the parallel field. This may account for the observed increased large excursions observed near the SI.

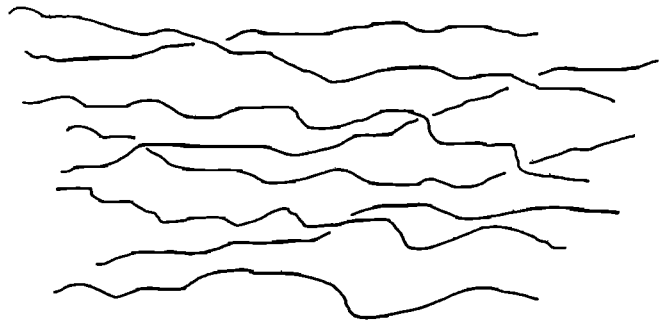

Figure 9. Field line mixing or random walk in a uniform flow.

Now clearly, other flow patterns may actually increase the perpendicular diffusion. For example, if we had an expansion rather than a compression in the last example above, this would occur. However, since a CIR is a compression surrounding a flow shear, conditions where a decrease occurs should be prevalent near a stream interface.

The 1-min Pioneer 11 field averages in the vicinity of the

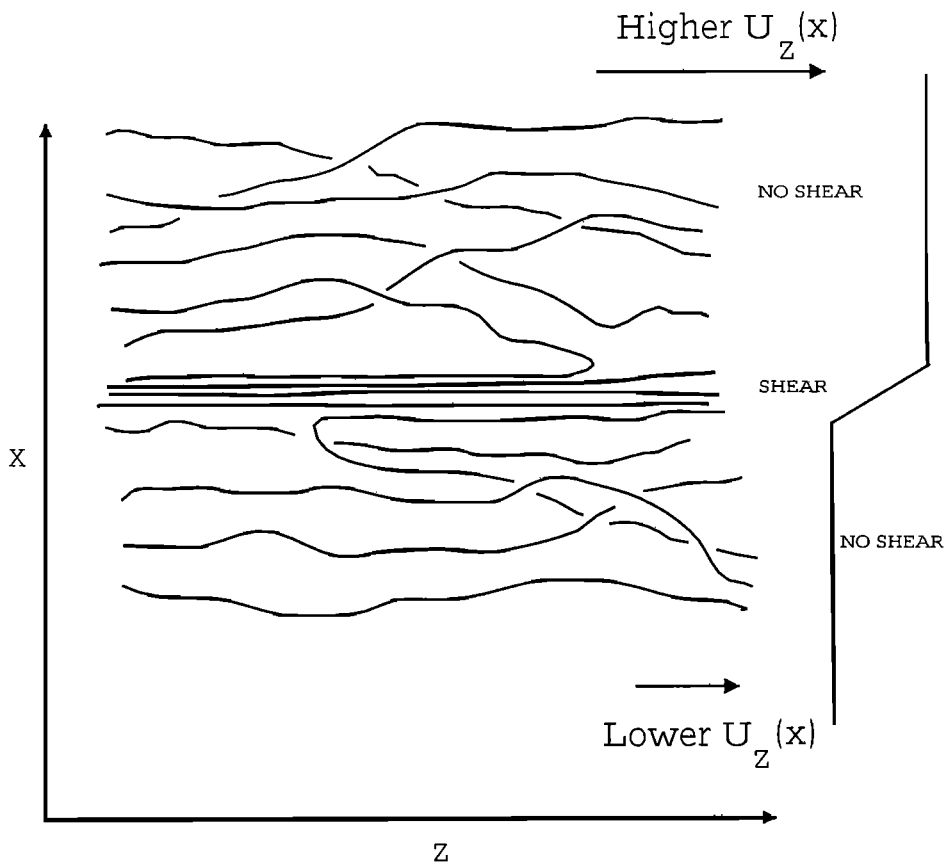

Figure 10. Illustration of the effect of region of velocity shear on a meandering magnetic field. The velocity vector U is in the z-direction, and depends only on x. In the region of shear, where $dU_z/dx > 0$, as illustrated, the parallel component of the magnetic field is amplified and the normal component is unchanged. The result is significantly less meandering, which depends on B_x/B_z within the shear layer.

SI shown in Figure 4 and the Pioneer and Ulysses planar structure in the TULs and CIRs shown in Figures 5a - 5d and 6a - 6d provide a basis for understanding the reduced random walk of field lines and the resulting reduced stochastic diffusion in the vicinity of the stream interface, as discussed above. The rapid variations in the magnetic field reduce the random walk of field lines and most likely are the result of a shear or a compression of the field near the stream interface. The planar magnetic structures also would inhibit the random walk of field lines and may be responsible for the step-like decreases in the energetic particle profiles for this event [see *Intriligator et al.*, 1995, Figure 2].

Figure 9 shows a sketch of the normal random walk of field lines. There are configurations where there is reduced random walk of field lines. For example, the field lines on both sides of a tangential discontinuity (the stream interface is a contact surface and usually a tangential discontinuity) will not be able to intermingle. As discussed above, a compression of the field (similar to steel wool) reduces the random walk of field lines. A region of velocity shear reduces the random walk of field lines as illustrated in Figure 10. The shearing of the field at the stream interface merits further discussion. In plasma data the abrupt increase in specific entropy at the SI is accompanied by both north/south and east/west deflections of the flow, which are indicative of shearing. The recent Ulysses-inspired insight on the polarward propagation of reverse shocks and the equatorward propagation of forward shocks [*Gosling et al.*, 1993; *Pizzo and Gosling*, 1994] is also consistent with a significant north-south shear in the vicinity of the SI. In the region of shear the parallel component of the magnetic field is amplified and the perpendicular component is unchanged. This results in significantly less meandering, which scales with $B_\perp/B_{11}$.

5. Effects of Shear and Compression on Perpendicular Transport

The perpendicular transport of energetic charged particles in a turbulent magnetic field is complicated. If we define perpendicular transport as transport in the direction normal to the average magnetic field, which is the only reasonable definition, then the perpendicular motion is composed, in general, of two quite different physical effects. First, the particles can move normal to the magnetic field lines themselves. Second, if the particle gyroradii are small compared with the largest scales in the turbulent magnetic field, the motion of the particles along the field lines will also contribute to the perpendicular motion, as the field lines themselves will, in general, have a component normal to the average field. This latter effect is called the effect of the field line random walk and is frequently more important than the movement of a particle from one field line to another. We concentrate on this here. A recent discussion of the field line random walk is given by *Kota and Jokipii* [2000].

Suppose the average magnetic field B_0 is in the z direction, so that the perpendicular directions are x,y. Let the randomly fluctuating magnetic field be in the x and y directions. The motion normal to the magnetic field in this case is proportional to the ratios B_x/B and B_y/B, where B is the magnitude of **B**. If $B_x/B \ll 1$, we may approximate the statistical random walk coefficient as

$$<(\Delta x)^2/\Delta z>_0 = (1/B_0^2) \int_0^\infty <B_x(z)B_x(z+\zeta)>d\zeta, \quad (1)$$

and similarly for $<\Delta y^2>/\Delta t$. This approximation will be used in what follows, although the conclusions are a bit more general.

The basic equation for the evolution of the magnetic field due to fluid motions at velocity **U**, in the ideal hydromagnetic approximation, is

$$\partial \mathbf{B}/\partial t = \nabla \times (\mathbf{U} \times \mathbf{B}), \quad (2)$$

which may be rewritten

$$\partial \mathbf{B}/\partial t + \mathbf{U} \bullet \nabla \mathbf{B} = \mathbf{B} \bullet \nabla \mathbf{U} - \mathbf{B} \nabla \bullet \mathbf{U}. \quad (3)$$

We look at two special cases that show most simply the effects of shear and compression on the random walk.

First, if compression or expansion occurs in an arbitrary direction (that is, $U = U_x(x)\,\hat{e}_x$), it may be shown from equation (2) that the y and z components of the magnetic field are changed in an amount directly proportional to the degree of compression (increase) or expansion (decrease), whereas the x component is unchanged. Clearly, then, the rate of random walk in the direction of compression or expansion is changed.

Specifically, if a compression occurs in the x direction by a factor $f > 1$, then $B_x \rightarrow f B_x$. That is, the x scales become a factor of f smaller and $dx \rightarrow dx/f$ whereas the y and z directions are unchanged. The random walk coefficient in the x direction becomes

$$<(\Delta x)^2/\Delta z> = (1/f^2) <(\Delta x)^2/\Delta z>_0 . \quad (4)$$

So the random walk is reduced by the factor f^2. The argument is the same for an expansion, except that $f < 1$ and the random walk is enhanced. Compression in other directions is not so simple, but as long as the compression direction has a significant component normal to the z axis, the result should be qualitatively the same.

Shear across a plane containing the average magnetic field can also be shown to reduce the field line random walk. Consider the shear illustrated in Figure 10. If the shear is written $\partial U_z/\partial x$, one can show that the values of B_x and B_y in a fluid element remain the same as the original values, while B_z in the fluid element changes at a rate proportional to the value of the shear. We have, for a system depending only on x,y and for which B_y is zero,

$$\partial B_x/\partial t + U_z\, \partial B_x/\partial z = 0, \quad (5)$$

$$\partial B_y/\partial t + U_z\, \partial B_y/\partial z = 0, \quad (6)$$

$$\partial B_z/\partial t + U_z\, \partial B_z/\partial z = B_x\, \partial U_z/\partial x + B_y\, \partial U_z/\partial y. \quad (7)$$

In the ideal hydromagnetic limit, B_x and B_y remain constant in a given fluid element and B_z will continually be stretched, eventually becoming larger and larger. This has two effects. Independent of the sign of B_x, the magnitude of B_z and hence B in the region of shear will eventually increase if $B_y = 0$.

Thus the ratio B_x/B_z will decrease. From (4) this then means that the random walk coefficient $[(\Delta x)^2/\Delta z]$ will decrease. Again, as in the case of compression, if the shear is not parallel to the average magnetic field, the effect still holds, but it is more complicated to evaluate quantitatively. Note also that the change in B_z continues without limit in this approximation.

We note one further interesting aspect of the effect of shear. From (7) we see that the change in B_z comes from B_x and B_y, which fluctuate in sign. Hence the sign of B_z will, in general, fluctuate between large positive and large negative values. This is similar to what is observed near the stream interface (see Figure 4). This will be studied more carefully in future work.

It is tempting to use the Pioneer and Ulysses observations to estimate the compression factor f in (4). For the Pioneer 11 data in Figure 5a, in the TUL (SI to SI + 12 hours) the magnetic field magnitude is the highest (most compressed) and almost reaches 6 nT. In the TUL the average field magnitude is 3.68 nT, and it is 0.29 nT in the free solar wind (day 99) so that f is 12.76. From (4) the random walk is reduced by a factor of f^2, a factor of 1/163 or > 2 orders of magnitude. For the Ulysses CIR, in the TUL the magnetic field magnitude reaches ~3 nT shortly after the SI and averages ~2 (2.06) nT. In the free solar wind it is 0.127 nT. So here again, as in the Pioneer 11 TUL case, the compression factor is substantial. Here f is 16.19, and the random walk is reduced by a factor of ~1/286. These reductions in the random walk in the TULs are consistent with those that *Intriligator and Siscoe* [1995] found were needed in the TUL. We note that in both the Pioneer 11 and Ulysses cases, if we were to estimate the compression factor for the whole CIR (instead of only the TUL), it would not be as large, since there is not as much compression behind the forward shock as there is immediately following the stream interface. Of course, effects other than compression can also increase the magnitude of B, so that we can say only that the measurements are consistent with compression.

6. Conclusions

We have presented evidence that supports reduced particle transport within two CIRs, particularly in the vicinity of the TUL (SI to SI + 12 hours). These include the following:

1. The 1-min magnetic field averages in the vicinity of the SI in the two CIRs reveal significant variations of the order of a few minutes in the B_N component of the field (Figures 3a - 3d and 4).

2. The TUL is a planar magnetic structure (Figures 5a - 5d and 6a - 6d).

3. The CIR is a planar magnetic structure (Figures 5a - 5d and 6a - 6d).

4. The random walk is reduced by a factor f^2 where f is the compression factor (equation (4)). On the basis of the data in Figures 5a - 5d and 6a-6d we estimate f^2 to be ~1/163 and 1/286 in the Pioneer and Ulysses TULs examined, respectively. This estimate is consistent with the results of *Intriligator and Siscoe* [1995], who concluded that a reduction in cross-field transport of ~2 orders of magnitude was needed near the stream interface (in the TUL) as compared to that of the free solar wind.

Thus we conclude that the effects of shear and compression reduce the particle transport in the CIRs, particularly in the TUL, and that there are several types of field variations that lead to this conclusion. These field variations are consistent with the reduced random walk of field lines and thus with the decrease in energetic particle intensity in the vicinity of the stream interface. It is tempting to speculate that step-like decreases in energetic particle intensity in the heliosphere in the vicinity of corotating merged interaction regions, global merged interactions, and other disturbances such as coronal mass ejections and traveling interplanetary disturbances may be associated with the reduced random walk of the field lines in these regions rather than solely with the change in magnetic field magnitude.

Acknowledgments. This paper is dedicated to the memory of John Simpson, our colleague and our friend. This work was supported in part by Carmel Research Center. T.S.H. was supported by PPARC (UK) grant GR/L29903. Work at Los Alamos was performed under the auspices of the U.S. Department of Energy with support from NASA.

Janet G. Luhmann thanks the referees for their assistance in evaluating this paper.

References

Clack, D., R. J. Forsyth, and M. W. Dunlop, Ulysses observations of the magnetic field structures within CIRs, *Geophys. Res. Lett.*, *27*, 625-628, 2000.

Conlon, T. F., The interplanetary modulation and transport of Jovian electrons, *J. Geophys. Res.*, *83*, 541-552, 1978.

Dwyer, J. R., G. M. Mason, J. E. Mazur, J. R. Jokipii, T. T. von Rosenvim, and R. P. Lepping, Perpendicular transport of low-energy-energy of corotating interaction region-associated nuclei, *Astrophys. J. Lett.*, *490*, L115-L118, 1997.

Gosling, J. T., S. Bame, D. J. McComas, J. L. Phillips, V. Pizzo, B. E. Goldstein, and M. Neugebauer, Latitudinal variation of the solar wind corotating stream interaction regions: Ulysses, *Geophys. Res. Lett.*, *20*, 2789, 1993.

Horbury, T. S., and J. Schmidt, Development and effects of turbulence in connection with CIRs, *Space Sci. Rev.*, *89*, 61-76, 1999.

Hu, Y. Q., Evolution of corotating stream structures in the heliospheric equatorial plane, *J. Geophys. Res.*, *98*, 13,201-13,214, 1993.

Intriligator, D. S., and G. L. Siscoe, Stream interfaces and energetic ions closer than expected: Analyses of Pioneer 10 and 11 observations, *Geophys. Res. Lett.*, *21*, 1117-1120, 1994.

Intriligator, D. S., and G. L. Siscoe, Cross-field diffusion in corotating interaction regions, *J. Geophys. Res.*, *100*, 21,605-21,612, 1995.

Intriligator, D. S., G. L. Siscoe, G. Wibberenz, H. Kunow, and J. T. Gosling, Stream interfaces and energetic ions, 2, Ulysses test of Pioneer results, *Geophys., Res. Lett.*, *22*, 1173-1176, 1995.

Jokipii, J. R., Cosmic ray propagation, 1, Charged particles in a random magnetic field, *Astrophys. J.*, *145*, 480, 1966.

Kota, J., and J. R. Jokipii, Velocity correlation and spatial diffusion coefficients of cosmic rays: compound diffusion, *Astrophys. J.*, *531*, 1067-1070, 2000.

Nakagawa, T., A. Nishida, and T. Saito, Planar magnetic structures in the solar wind, *J. Geophys. Res.*, *94*, 11,761-11,775, 1989.

Neugebauer, M., D. R. Clay, and J. T. Gosling, The origins of planar magnetic structures in the solar wind, *J. Geophys. Res.*, *98*, 9383-9389, 1993.

Palmer, I. D., and J. T. Gosling, Shock-associated energetic proton events at large heliocentric distances, *J. Geophys. Res.*, *83*, 2037, 1978.

Pizzo, V. J., The evolution of corotating stream fronts near the ecliptic plane in the inner solar system, 1, Two-dimensional fronts, *J. Geophys. Res.*, *94*, 8673-8684, 1989.

Pizzo, V. J., and J. T. Gosling, 3-D simulation of high-latitude interaction regions: Comparison with Ulysses results, *Geophys. Res. Lett.*, *21*, 2063-2066, 1994.

Siscoe, G., and D. S. Intriligator, Three views of two giant streams: Aligned observations at 1 AU, 4.6 AU, and 5.9 AU, *Geophys. Res. Lett.*, *20*, 2267-2270, 1993.

R. J. Forsyth and T. S. Horbury, The Blackett Laboratory, Imperial College, London SW7 2BZ, England, United Kingdom

J. T. Gosling, MS D466, Los Alamos National Laboratory, Los Alamos, NM 87545.

D. S. Intriligator and J. M. Intriligator, Space Plasma Laboratory, Carmel Research Center, P.O. Box 1732, Santa Monica, CA 90406.

J. R. Jokipii, Department of Planetary Sciences, University of Arizona, Space Sciences Bldg.,Tucson, AZ 85721.

H. Kunow and G. Wibberenz, Extraterrestrische Physik, Institut fur Experimentelle und Angewandte Physik, Universitat Kiel, D-24118, Kiel, Germany.

(Received March 2, 2000; revised October 24, 2000; accepted November 15, 2000.)